POLITECNICO
MILANO 1863

SCUOLA DI INGEGNERIA INDUSTRIALE
E DELL'INFORMAZIONE

Venus Express (VEX) - Group 05

Report on the analysis, reverse engineering and sizing of the interplanetary mission

Authors:

NAME	SURNAME	PERSON CODE
Damiana	Irrera	10578918
Riccardo	Picozzi	10620335
Davide	Rosato	10618468
Jason	Spinelli	10618465
Paolo	Tognola	10618360
Davide	Zamblera	10612897

Course: Space Systems Engineering and Operations
Professor: Michelle Lavagna
Academic Year: 2021-22

Abstract

This report aims to analyse the Venus Express (VEX) mission through the description of the spacecraft's subsystems and the explanation of the main design and operational choices implemented. The subsystems have been studied with the reverse-engineering method, starting from the available data, to double-check their technological features and quantify their capabilities. Moreover, the main requirements of each subsystem have been drafted, checking their correlation and cross-checking their mutual validity.

Contents

List of Symbols

Variable	Description	SI unit
ΔV	Budget of the mission	[km/s]
ΔV_{left}	delta-V left after Main Engine insertion	[m/s]
ϵ_{venus}	Emissivity of Venus	[-]
γ	Gas cp/cv ratio	[-]
μ	Gravitational constant of Venus	[km^3/s^2]
Ω	Right ascension of the ascending node	[deg]
ω	Argument of periapsis	[deg]
ρ_{fuel}	Fuel density	[kg/dm^3]
ρ_{ox}	Oxidizer density	[kg/dm^3]
σ	Boltzmann's constant	[W m^{-2} K^{-4}]
θ	Slew angle	[deg]
a	Semi-major axis	[km]
a_f	Albedo factor	[-]
A_c	Cross section area of the s/c	[m^2]
A_{rad}	Area of the radiators	[m^2]
A_s	Area of the spacecraft exposed to SRP	[m^2]
A_{sc}	Area of the s/c that is irradiating with the surroundings	[m^2]
c_g	Center of gravity of the s/c	[m]
c_{pa}	Center of aerodynamic pressure	[m]
c_{ps}	Center of solar pressure	[m]
c_T	Thrust coefficient	[-]
C_d	Drag coefficient	[-]
e	Eccentricity	[-]

Variable	Description	SI unit
$\boldsymbol{F_s}$	Solar radiation constant	[W/m^2]
$\boldsymbol{F_{thr}}$	Thrust generated by the thrusters	[N]
$\boldsymbol{g_0}$	Earth's gravity acceleration	$[m/s^2]$
$\boldsymbol{H}$	Momentum stored by the RW	[Nms]
$\boldsymbol{i}$	Inclination	[deg]
$\boldsymbol{I_{max}}$	Maximum principal inertia moment	[kg m^2]
$\boldsymbol{I_{min}}$	Minimum principal inertia moment	[kg m^2]
$\boldsymbol{I_{sp}}$	Specific impulse	[s]
$\boldsymbol{I_{sp,thr}}$	Specific impulse of the thrusters	[s]
$\boldsymbol{J}$	Cost function	[m/s]
$\boldsymbol{L_{arm}}$	Arm wrt the CG of the thrusters	[m]
$\boldsymbol{m_0}$	Total initial mass	[kg]
$\boldsymbol{m_f}$	Final mass	[kg]
$\boldsymbol{m_{He}}$	Helium mass	[kg]
$\boldsymbol{m_{prop}}$	Propellant mass	[kg]
$\boldsymbol{m_{ox}}$	Oxidizer mass	[kg]
$\boldsymbol{M_{dry}}$	Dry mass of the s/c	[kg]
$\boldsymbol{M_{p,off}}$	Propellant mass needed for the off-loading	[kg]
$\boldsymbol{n}$	Number of thrusters involved	[-]
$\boldsymbol{O/F}$	Mixture ratio	[-]
$\boldsymbol{P_{in}}$	Tank internal pressure	[bar]
$\boldsymbol{q}$	Reflectance factor	[-]
$\boldsymbol{\dot{q}_a}$	Albedo heat flux	[W/m^2]
$\boldsymbol{\dot{q}_{IR}}$	Infrared heat flux	[W/m^2]
$\boldsymbol{\dot{q}_{sun}}$	Sun heat flux at Venus	[W/m^2]
$\boldsymbol{\dot{q}_0}$	Sun heat flux at Earth	[W/m^2]
$\boldsymbol{\dot{Q}_{int}}$	Power generated by the s/c (electronics, etc.)	[W]
$\boldsymbol{\dot{Q}_{IR}}$	Infrared heat-trasfer	[W]
$\boldsymbol{\dot{Q}_{heat}}$	Power generated by the heaters	[W]

Variable	Description	SI unit
$\boldsymbol{r_{earth}}$	Orbital radius of Earth wrt Sun	[km]
$\boldsymbol{r_{sc}}$	Orbital radius of the s/c	[km]
$\boldsymbol{r_{venus}}$	Orbital radius of Venus wrt Sun	[km]
$\boldsymbol{R}$	Orbit radius	[km]
$\boldsymbol{R_{apo}}$	Radius at apocenter	[km]
$\boldsymbol{R_{He}}$	Helium gas constant	[J/K*kg]
$\boldsymbol{R_{per}}$	Radius at pericenter	[km]
$\boldsymbol{R_{venus}}$	Radius of Venus	[km]
$\boldsymbol{t_{pulse}}$	Thruster desaturation impulse duration	[s]
$\boldsymbol{t_{slew}}$	180° slew duration	[s]
$\boldsymbol{T}$	Orbit period	[h]
$\boldsymbol{T_a}$	Aerodynamic torque	[Nm]
$\boldsymbol{T_c}$	Combustion chamber temperature	[K]
$\boldsymbol{T_{cold}}$	Worst case scenario cold temperature	[K]
$\boldsymbol{T_d}$	Total disturbances torque	[Nm]
$\boldsymbol{T_{eff}}$	Effective radiating temperature of Venus	[K]
$\boldsymbol{T_g}$	Gravity gradient torque	[Nm]
$\boldsymbol{T_{hot}}$	Worst case scenario hot temperature	[K]
$\boldsymbol{T_{max}}$	Maximum allowable s/c temperature	[K]
$\boldsymbol{T_{min}}$	Minimum allowable s/c temperature	[K]
$\boldsymbol{T_{RW}}$	Torque of each Reaction Wheel	[Nm]
$\boldsymbol{T_{sp}}$	Solar pressure torque	[Nm]
$\boldsymbol{T_{thr}}$	Torque generated by the thrusters	[Nm]
$\boldsymbol{U}$	Nodal internal energy of the spacecraft	[J]
$\boldsymbol{v}$	Orbital speed	[m/s]
$\boldsymbol{V_{fuel}}$	Fuel volume	[L]
$\boldsymbol{V_{ox}}$	Oxidizer volume	[L]
$\boldsymbol{V_{prop}}$	Propellant volume	[L]

1 | Introduction

Venus Express (VEX) [5] is a European Space Agency (ESA) mission designed to perform a global investigation of the Venusian atmosphere and of the plasma environment. In this work, the reverse engineering of the mission has been analysed.

The spacecraft is based on the Mars Express bus to maximize the use of Mars Explorer Mission components, however, it has been modified to make it more suited in order to operate near Venus.

Venus Express was launched on 9 November 2005, and after an interplanetary cruise that lasted 153 days, in April 2006, the spacecraft was inserted in an elliptical polar orbit around Venus, with an orbital period of 24 hours. The nominal mission lasted 500 days, until 19 September 2007. After that, ESA decided to extend the mission several times over the years, in order to increase the amount of data and better understand Venus and its characteristics. Venus Express worked until 16 December 2014, when ESA declared its propellant completely depleted.

The purpose of this paper is to perform a review of the mission design of the Venus Express; by doing a retrospective evaluation, it is possible to investigate the design choices made by ESA, so that it's possible to learn from the experience and predict possible improvements for a future mission.

The mission analysis study is conducted in all its phases, such as in proximity to Earth, during the interplanetary journey, and once in Venus orbit; the various design choices related to the surrounding environment will be considered. Subsequently, an in-depth study regarding all subsystems of the spacecraft is performed, evaluating the reasons behind the design choices and possible refinements.

2 | Scientific payload

The scientific payload is made up by seven instruments which are briefly described in tab.2.1 and in the following subsection.

Instrument	Instrument purpose
ASPERA-4	Neutral and ionized plasma analysis
MAG	Magnetic field measurements
SPICAV	Atmospheric spectrometry by star or Sun occultation
VeRa	Radio sounding of atmosphere and ground surface
VIRTIS	Spectrographic mapping of atmosphere and surface
PFS	Atmospheric vertical sounding by infrared Fourier spectroscopy
VMC	Ultraviolet and visible imaging

Table 2.1: Scientific payload

2.1. ASPERA-4

ASPERA-4 (Analyser of Space Plasmas and Energetic Atoms) studies energetic neutral atoms (ENAs), ions and electrons. It is based on the Mars Express ASPERA-3.

The experiment is designed to:

- Investigate the interaction between the solar wind and the atmosphere of Venus;
- Characterize the impact of plasma processes on the atmosphere;
- Determine the global distribution of plasma and neutral gas;
- Identify the mass composition and quantitatively characterise the flux of the out flowing atmospheric materials;
- Investigate the plasma domains of the near Venus environment;
- Provide undisturbed solar wind parameters.

2.2. MAG

The Magnetometer instrument is designed starting from the ROMAP of the Rosetta Lander and it is used to make measurements of magnetic field strength and direction in order to:

- Provide the magnetic field data for any combined field, particle and wave studies such as lightning and planetary ion pickup processes;
- Map with high time resolution the magnetic properties in the magnetosheath, magnetic barrier, ionosphere, and magnetotail;
- Identify the boundaries between the various plasma regions;
- Study the interaction of the solar wind with the atmosphere of Venus.

2.3. SPICAV

SPICAV (Spectroscopy for Investigation of Characteristics of the Atmosphere of Venus) is an imaging spectrometer for ultraviolet and infrared radiation. SPICAV is derived from the SPICAM instrument flown on Mars Express, which was equipped with two channels, one for ultraviolet wavelengths and one for infrared. An additional channel (SOIR, Solar Occultation at Infrared) has been added for Venus Express, to observe the Sun through Venus's atmosphere at infrared wavelengths.

2.4. VeRa

VeRa (Venus Radio Science) is a radio sounding experiment that is used to examine the ionosphere, atmosphere and surface of Venus by means of radio waves transmitted from the spacecraft, passed directly through the atmosphere or reflected off the planet surface and received by a ground station on Earth. It is derived from the Rosetta's RSI and it is designed to:

- Perform radio sounding of the Venus ionosphere from an altitude of 80 kilometres to the ionopause (300 - 600 km, depending on solar wind conditions);
- Perform radio sounding of the neutral atmosphere from the cloud layer (35 - 40 km) to an altitude of around 100 kilometres;
- Determine the dielectric characteristics, roughness and chemical composition of the planetary surface;

- Study the solar corona, extended coronal structures and solar wind turbulence during the inferior and superior solar conjunctions of Venus.

2.5. VIRTIS

VIRTIS (Visible and Infrared Thermal Imaging Spectrometer) is an imaging spectrometer that operates in the near ultraviolet, visible and infrared parts of the electromagnetic spectrum (0.25 to 5 μm wavelength range). The instrument has a variety of operating modes that cover a range of observations from pure high-resolution spectrometry to spectro-imaging. VIRTIS allows the analysis of all layers of the atmosphere and the clouds therein, the making of surface temperature measurements and the study of surface -atmosphere interaction phenomena. VIRTIS is based on the visrtis instrument used in the Rosetta mission.

2.6. PFS

PFS is a Planetary Fourier Spectrometer which is based on the PFS of the Mars express and it is designed to:

- Perform global, long-term monitoring of the three-dimensional temperature field in the lower atmosphere (from cloud level up to 100 km);
- Measure the concentration and distribution of known minor atmospheric constituents;
- Search for unknown atmospheric constituents;
- Determine, from their optical properties, the size, distribution and chemical composition of atmospheric aerosols;
- Investigate the radiation balance of the atmosphere and the influence of aerosols on atmospheric energetics;
- Study global circulation, mesoscale dynamics and wave phenomena;
- Analyse surface to atmosphere exchange processes.

2.7. VMC

VMC (Venus Monitoring Camera) is a wide angle, multi-channel CCD camera that, using four narrow band filters, operates in the ultraviolet, visible and near infrared spectral ranges. It comes from Mars Express (HRSC/SRC) and Rosetta (OSIRIS) missions and

it is needed to fulfil the following goals:

- Perform support imaging (supply a global imaging context for data from the other instruments);
- Facilitate the study of dynamic processes in the atmosphere of Venus by means of global, multi-channel imaging;
- Permit the study of the distribution of the unknown UV absorber at the cloud tops;
- Monitor the ultraviolet and visible wavelength airglow and its variability as a dynamic tracer;
- Map the surface brightness distribution and search for volcanic activity.

3 | Environment

3.1. High solar radiation

Given the proximity of Venus to the Sun, it is necessary to consider the disturbances caused by our star on the spacecraft. Particularly, during the Earth-Venus interplanetary transfer and its permanence on the planet's orbit, the spacecraft is hit by high solar radiation, which can cause damage to several components of the spacecraft, such as electronic instruments or telecommunication components, as much as some parts of the propulsion and power system, such as cryogenic fuel storage and solar panels. Therefore, it is necessary during the design phase to consider a suitable payload configuration and to make sure that specific instruments are not directly hit by the sun's rays and function properly throughout the mission.

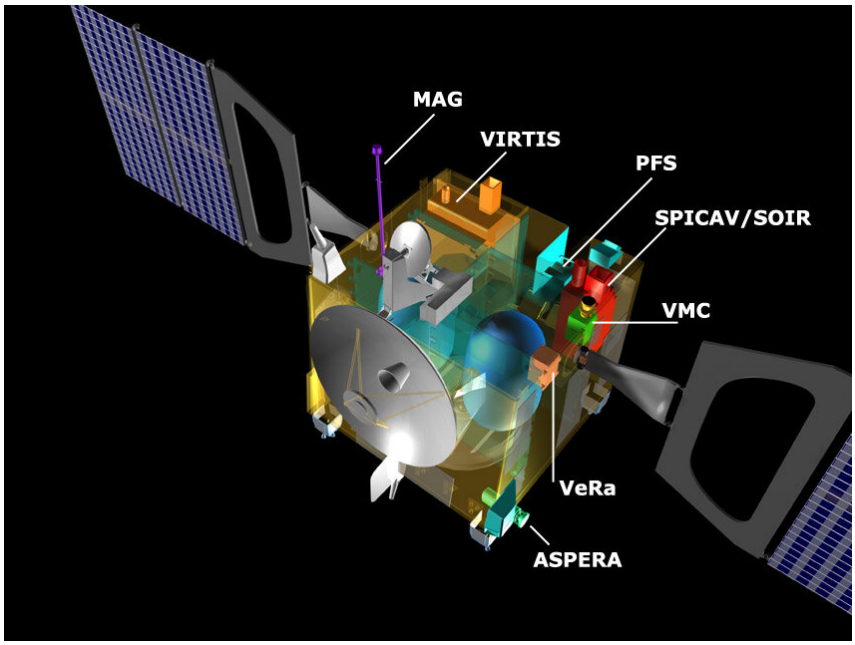

Figure 3.1: Payload configuration

3.2. Third body perturbation

Once the spacecraft arrived in the proximity of Venus, the Sun's third body perturbation needs to be considered, in other terms the direct gravitational attraction of the Sun on the spacecraft's operational orbit. Particularly, it affects perigee altitude, which would increase by more than 150km. In this way, it would not be possible to have the right study of Venus's atmosphere, which is one of the mission objectives. Moreover, considering the long-term evolution of the orbit, the argument of the perigee would also be affected by modification; it diminishes about 9 deg in 1000 days.

In order to satisfy the requirement ENV-07 in table 3.1, it has been chosen to perform a series of apocenter-pericenter-apocenter maneuvers whenever the perigee altitude goes above 400 km.

3.3. Requirements

ID	Requirements
ENV-01	All the components shall be able to work under high temperature conditions or be covered from direct Sun illumination
ENV-02	The spacecraft surface shall be able to contain heat absorption
ENV-03	The heat sink used by instruments that require cryogenic temperature must be covered always from the Sun illumination
ENV-04	Main engine and nozzle shall mostly avoid direct Sun illumination to avoid solar heat absorption
ENV-05	The spacecraft solar arrays shall be able to resist high temperature
ENV-06	The spacecraft antennas used to communicate with the ground must be covered from illumination. Their number shall be redundant to always allow communication
ENV-07	The s/c shall be able to perform trajectory maneuvers to maintain the pericenter operational orbit between 200 km and 400 km, and the argument of perigee around 90 degrees

Table 3.1: Environment requirements

4 | Mission analysis

4.1. Near Earth operations

Venus Express was launched on 9 November 2005, at 3:33 UT by a Soyuz-Fregat rocket from the Baikonur Cosmodrome in Kazakhstan. The launch features are obtained through an optimization problem based on a fmincon multishooting algorithm. In particular, after the first phase where the launcher is affected by the gravity turn, the control phase starts by applying the thrust vector control. The problem is solved by finding the solution of $\dot{\vec{x}} = f(\vec{x}, \vec{u})$ where $\vec{x}$ is the state and $\vec{u}$ is the control vector needed to minimize the cost function defined as $J = \sum w_i g_i$. The target orbit considered is shown in tab.4.1.

Figure 4.1 shows the profile of the mission after the launch till the fregat main burn where the Fregat-Venus Express composite is placed into an almost circular parking orbit. After a coast phase of about 70 minutes in the low Earth orbit, a second Fregat engine burn, lasting 16 minutes, moved the combined craft from the parking orbit onto an escape trajectory, after which the Fregat stage and Venus Express separated.

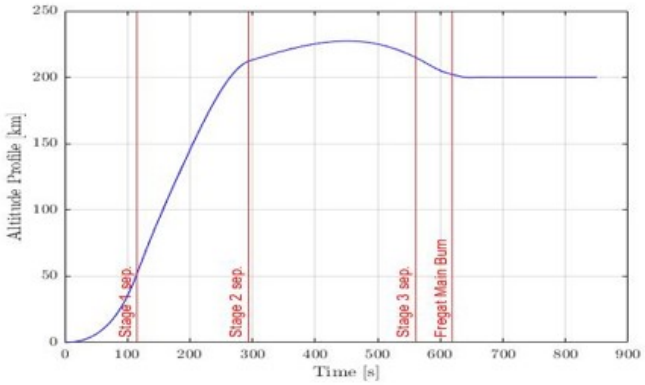

Figure 4.1: Burn stages

a [km]	e [-]	i [deg]	Ω [deg]	ω [deg]
6578	0	51.79	115.83	51.79

Table 4.1: Target orbit

4.2. Interplanetary operations

After launch and separation the spacecraft spends various months in an interplanetary leg where small correction maneuvers are performed. The main results from this analysis are the launch date and arrival date that minimize propellant consumption. The analysis is performed via a grid search on initial and final time and Lambert is used to determine initial and final velocities, afterwards a gradient search is performed on the minimum of the grid. This preliminary analysis, doesn't account for near earth maneuvers or Venus insertion, the true ΔV is much smaller. The resulting dates are still the optimal ones, since the dynamic of the problem do not change, when performing more complete and complex simulations. The results are contained in table 4.2, where literature results are also reported, and shown in fig. 4.2 [6]. The trajectory is shown in fig. 4.3, Earth and Venus are also visible, and the figure highlights how the planets at the initial and final times are in opposition, similar to a Hohmann transfer, which is the ideal optimal maneuver for two impulse transfers.

Table 4.2: Interplanetary leg results

-	Departure Date	Arrival Date
Analysis	2005/11/02 10:39:57	2006/04/09 11:35:20
Literature	2005/10/28 6:22:43	2006/04/05 11:03:28

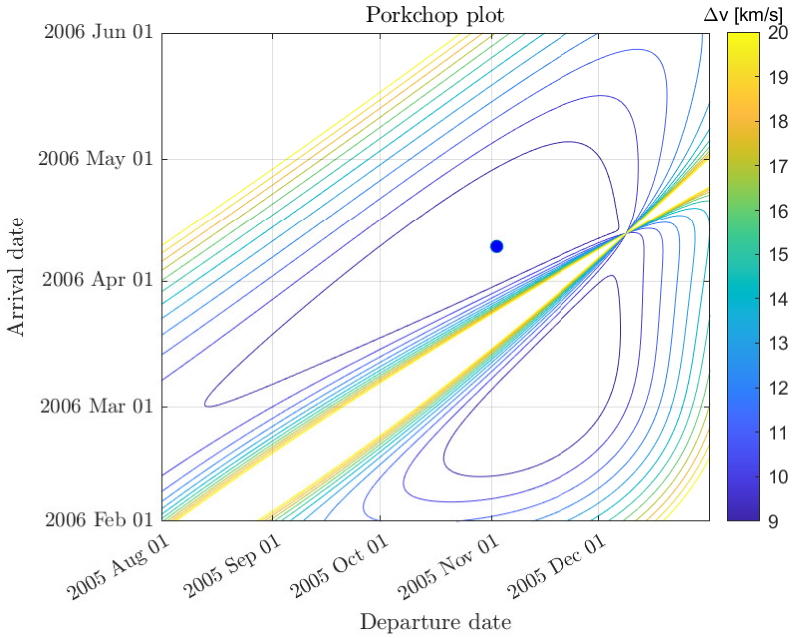

Figure 4.2: Porkchop plot of Interplanetary leg

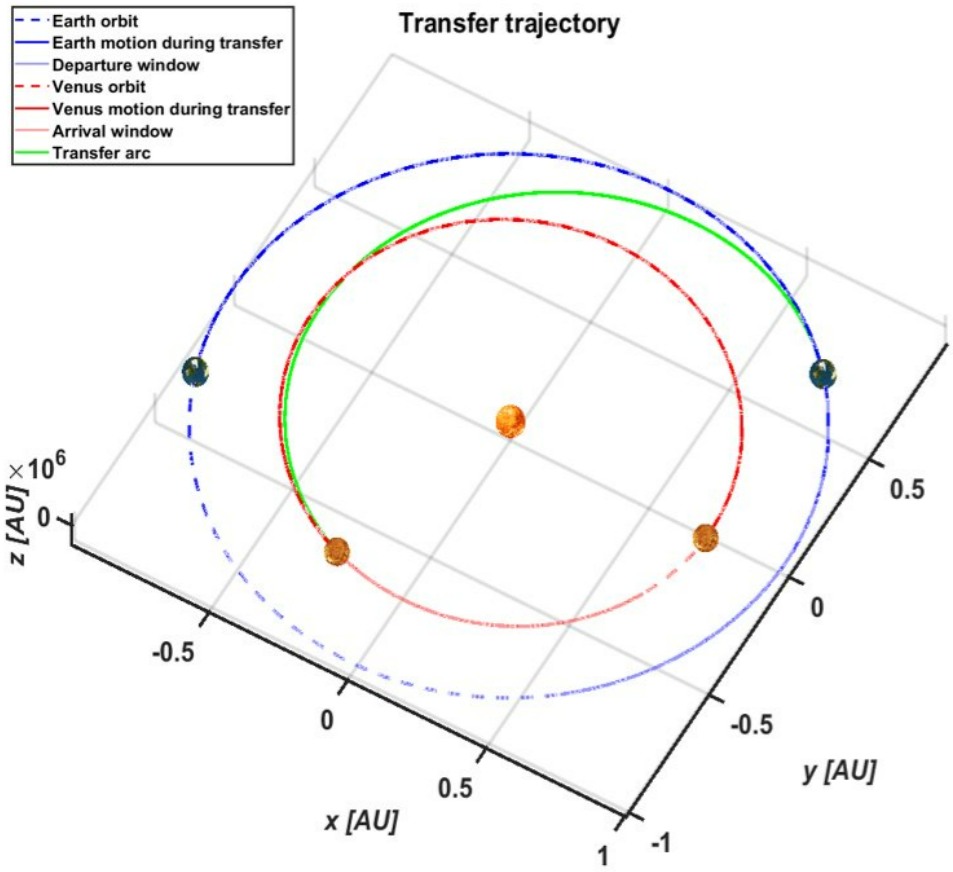

Figure 4.3: Interplanetary trajectory

The only orbital maneuver events of this phase are the TCMs, Trajectory Correction Maneuvers, the main ones were TCM-2 which was necessary to trim the spacecraft trajectory after the Main Engine Calibration maneuver and the TCM-3 executed in March to tune the arrival hyperbola for VOI. The total ΔV used for these events can be estimated to be around 5 m/s.

4.3. Near Venus operations

At the terminal part of the interplanetary leg begins the series of near Venus operations, consisting mainly in the orbital insertion. A long initial Main Engine burn is able to successfully change the orbit from hyperbolic to elliptical. Following that, a series of Apoapsis and Periapsis lowering maneuvers, fig. 4.4 are able to get the orbit into the desired final polar shape, table 4.3. The total calculated ΔV expenditure is of 1590 m/s, of which 1250 m/s are dedicated to the Main Engine burn. The difference between the analysis and the real total ΔV of the mission is of only 7 m/s.

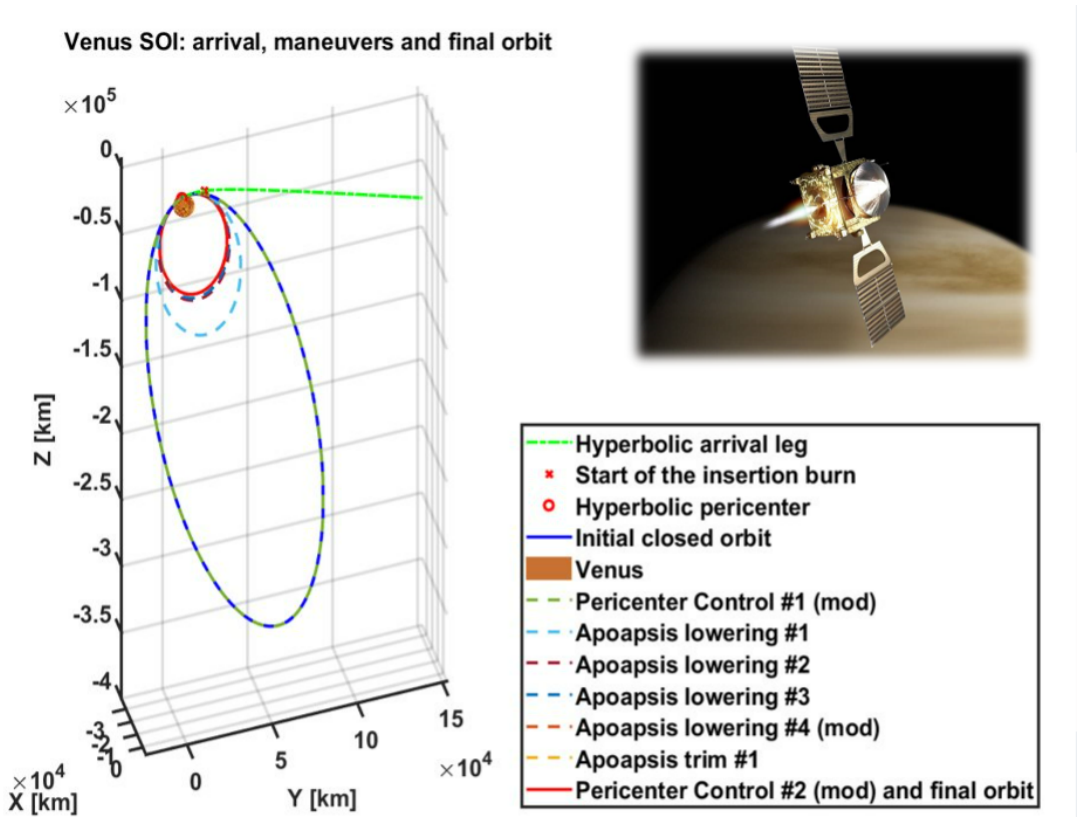

Figure 4.4: Series of orbital maneuvers completed for the insertion

a	e	i	Ω	ω	T
39196 km	0.8392	90°	103.94°	101.05°	24h

Table 4.3: Final orbit parameters

4.4. Requirements

Through our reverse engineering the mission requirements have been respected, table 4.4.

ID	Requirements
MA-01	The final operational orbit around Venus shall have inclination of about 90 degrees
MA-02	The spacecraft shall be capable of maintaining the operational orbit pericenter altitude between 250 km and 400 km
MA-03	The final orbit around Venus shall have a 24h period

Table 4.4: Mission requirements

5 | Chemical Propulsion System

5.1. Introduction and System Level Requirements

The propulsion subsystem for the Venus Express mission must meet the mission analysis requirements to achieve a final operational orbit around Venus and prevent environmental forces from disrupting it during the whole life cycle. These general objectives are then achieved by validation of the system level requirements in table 5.1.

ID	Requirements
PROP-01	The PS shall provide a ΔV insertion maneuver of 1250 m/s
PROP-02	The PS shall control orbit perturbation on the height at pericenter in the range 250 km to 400 km
PROP-03	The PS shall provide control of the interplanetary leg to maintain the coordinates at B-plane in the allowable range
PROP-04	The PS shall provide a correction maneuver of magnitude comparable to the maximum required by the worst case condition. This condition is determined by the standard deviation obtained by the covariance matrix on position and velocity known from the launcher provider.

Table 5.1: PS requirements

The system will be also influenced by the legacy of the use of an Eurostar 3000 base system, though the main architecture and operations remain the same.

5.2. Choice of the system architecture

The system is designed for a dual phase use. The first phase uses the ME, providing 416N of thrust, for insertion into Venus orbit and comprises also the interplanetary leg, the second consists in keeping the orbital parameters of the operational orbit in check. While

in the first stage of the mission a regulated pressure utilization is necessary to maintain a certain pressure in the ME combustion chamber, in the second phase the utilization of solely the thrusters makes a blowdown mode more appealing. The passage from one mode to another is executed after the ME insertion firing and consist in the deactivation of the regulated pressure valves and the close off the ME propellant distribution section. The passage between one mode to another must be carried out before the propellant in the main tanks is reduced to 60 kg, after this point the main engine cannot be used anymore, the RCT, providing 10N thrust each, are then employed to conclude the remaining maneuvers. Since the RCT are used also for attitude control the spacecraft employs 4 of them, with other 4 redundant ones to avoid critical failures.

The main PS events, and corollary informations about them are are contained in table 5.2, these were taken from the real mission and confronted with the reverse engineering values from the mission analysis.

Table 5.2: Propellant budget table

Maneuver	ΔV [m/s]	Engine
Launcher Injection Correction	15.0	ME
Interplanetary Navigation	5.0	ME
RCT Check out	1.0	RCT
ME Check out	3.0	ME
Venus Orbit Insertion	1290	ME
Lowering Apocenter 1st	280	ME
Lowering Apocenter 2nd	30	RCT
Orbit Control	70	RCT
Total	1694	-

5.3. Choice of the propellant

Since the mission consists of a planetary exploration mission the choice of the propellant couple is clearly oriented towards a bi-propellant hypergolic storable combination. The final decision was to use a monomethyl hydrazine (MMH) as the fuel and mixed oxides of nitrogen with 3% nitric oxide (MON-3) as the oxidant. This is a common couple for planetary missions, the relevant properties of this couple for the mission are discussed in the following.

The couple has long storability properties, with no changes in the purity of the compounds. This is compatible with the need to be preserved for a mission of at least 2 Earth years.

Another advantage of the couple is hypergolicity, which is beneficial for the second phase

of the mission where multiple re-ignition are necessary. This avoid use of igniters which would get otherwise usured by the repetitive engine cycles needed to complete the Venus insertion maneuver and to maintain a stable orbit.

At last the couple presents a good range of utilization temperatures which even though it does not eliminate the need for a specialized thermal control it makes this control of less energetic importance over the overall expenditures

A major disadvantage of this choice is with regard to the safety of the propellants. Monomethyl hydrazine vapors have a wide range of explosive limits and high reactivity with many materials, then strict adherence to the handling protocol is necessary. The compound is also toxic and carcinogenic. This increase the risks for the land personnel and the costs for the correct handling of the chemical compounds before the start of the mission.

5.4. CEA analysis

The choice of the system oxidizer to fuel ratio lies in performance measures such as I_{sp} and C_T, an other useful information on the design come from the chamber temperature T_{chamb}. The evaluation of these quantities was made with the CEA software. The simulation was carried out with an expansion model that freeze the chemical reaction after the throat, Bray model, this assumption is reasonable since the combustion involves the production of water vapour. [8]

The data to initialize the simulation are reported in table 5.3, while the results are shown in fig. 5.1. Note that the temperatures vary slightly from those of the real system for absence of database information in the real conditions, still the results are not expected to be very different for this simplification.

Reactant	WT Fraction	Temperature K
CH_6N_2(L)	1 (fuel)	298.15
N_2O_4(L)	0.97 (ox)	298.15
NO	0.03 (ox)	273.15

Table 5.3: Data for CEA simulation

Considering that the real mission used an O/F=1.67, it can be inferred that the choice of this ratio was not dictated by a requirement on maximum performances. The choice could be dictated by considerations on the maximum temperatures the combustion chamber can achieve without structural damage or being generated by other subsystems or mission requirements.

The condition from literature in which the RCT were used are also visible, the O/F is reduced to 1.54, and the performance are reduced accordingly.

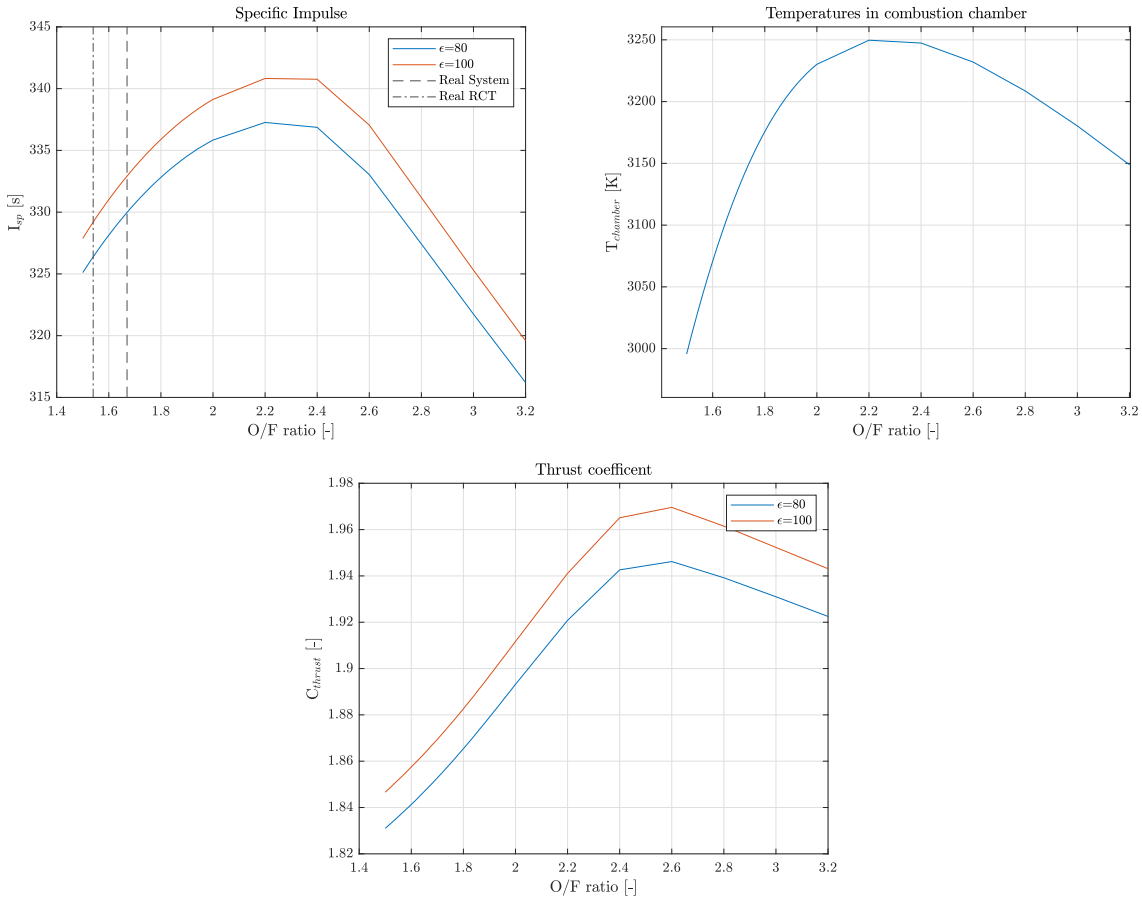

Figure 5.1: Results of NASA CEA analysis

5.5. Sizing of propellant masses

Since the preliminary determination of the ΔV closely match the real data in table 5.2, the sizing is considered only for this case. The propellant masses are determined using Tsiolkovsky rocket equation in eq. (5.1).

$$\Delta V = I_{sp} g_0 \log\left(\frac{m_0}{m_f}\right) \tag{5.1}$$

The sizing started by a determination of the final dry mass by a statistical interpolation of this variable using values from similar missions with different mass payloads, the interpolation was done assuming a payload of 93kg. The final dry mass is then obtained as 762kg from fig. 5.2, the specific impulse is determined as 330s from CEA analysis.

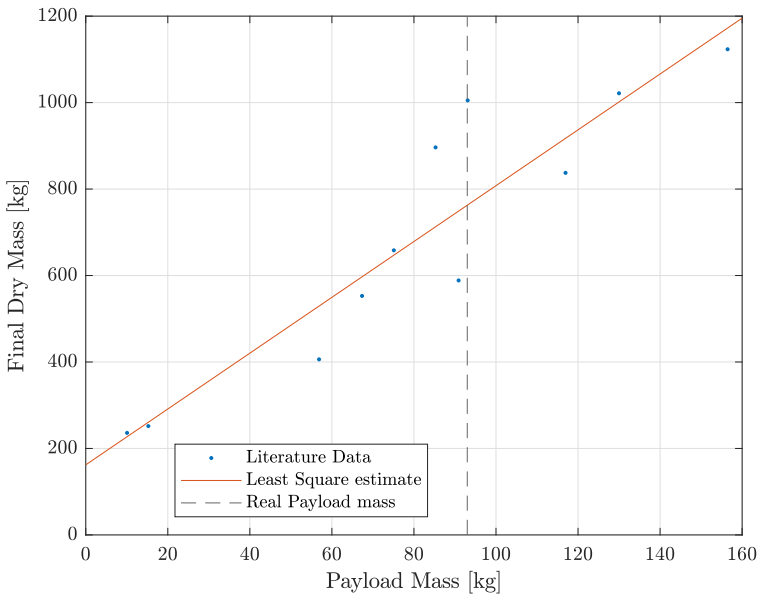

Figure 5.2: Determination of final dry mass

Then applying repeatedly Tsiolkovsky the whole mass budget for the propellants was determined, the results are reported in table 5.5, the final mass value amounts to 1287.3kg, while the value found in the literature is 1270kg, the difference amount is within the margin and the check is satisfactory.

Masses [kg]	Before ME burn	ME burn	Apocenter Lowering	Orbit Control
Propellant Mass	5.443	376.495	115.147	27.564
Cumulative Mass	768.099	1144.594	1259.742	1287.306

Table 5.4: Mass sizing

5.6. Tanks and feeding system sizing

The next sizing step is to use the determined propellant mass of 525kg and determine a sizing for the mass of oxidizer and fuel and the corresponding tanks and pressurization system. The necessary steps are described in the eq. (5.2), the masses were already increased by 3% due to ullage volumes, also the volumes were decreased for the 60.1kg of propellants which remains for the blowdown mode. The results consists of 2 tanks of 233L for fuel and oxidizer, by applying the necessary margins this results are compatible with the real one of 267L found in [2].

$$m_f = \frac{m_{prop}}{1 + O/F} = 196.498kg \tag{5.2a}$$

$$m_{ox} = m_{prop} - m_f = 328.152kg \tag{5.2b}$$

$$V_{ox} = \frac{m_{ox}}{\rho_{ox}} - V_{blowdown} = 233 - 25.9 = 204.4L \tag{5.2c}$$

$$V_{fuel} = \frac{m_{fuel}}{\rho_{fuel}} - V_{blowdown} = 230 - 25.6 = 207.17L \tag{5.2d}$$

$$V_{prop} = V_{ox} + V_{fuel} = 412L \tag{5.2e}$$

The propellant feeding strategy is chosen as pressure fed, as high power requirements and high vibrations of a pump fed systems are not compatible with the requirements for a satellite spacecraft. The pressurant is chosen as helium, the alternative would be nitrogen, this choice has the benefit of a reduced pressurant mass, with the downside of more leakage problems.

Then it was assumed that the final pressure will be 24bar, slightly higher than the pressure at which the ME works due to pressure losses and it was considered from literature that the initial pressure of the pressurant gas must be in the order of 10 higher than the final one, in this case the value of 275bar was chosen. Then considering the conservation of energy and adiabatic flow, due to the fast dynamics of the firing, eq. (5.3) was used to compute pressurant mass and pressurant volume. The result of a tank with volume 34.37L is compatible with the value of 35.5L in [ref]. By assuming also a Titanium alloy for the spherical pressurant tank, a estimate of the mass can be obtained.

$$m_{He} = \frac{p_{prop}}{V_{prop}} \left(\frac{\gamma}{1 - p_{fin}/p_{in}} \right) = 15kg \tag{5.3a}$$

$$V_{He} = \frac{m_{He} R_{He} T}{p_{in}} = 34.37L \tag{5.3b}$$

5.7. Mass breakdown and Electric consumption

The sizing can be completed by determining the total weight of the subsystem and the total electric consumption, when data is not determinable with the available informations the values are searched from the literature and similar missions.

Piece	Number	Mass [kg]	Power consumption [W]
Filters	4	0.284	-
Flow Control Valve	2	0.3	38.4
Fill and Drain Valve	11	0.09	-
Fill and Vent Valve	9	0.09	-
Latch Valve	2	0.545	12.9
Non Return Valve	4	0.09	-
Pressure regulator	2	2.3	61.4
Pressure Transducer	4	0.5	20
Pyrotechnic Valve	17	0.160	-
Thruster Latch Valve	8	0.545	12.9
Helium Pressurant Tank	1	14.4	-
MMH Tank	1	10.8	-
NTD Tank	1	10.8	-
Main Engine	1	3.6	-
Reaction control thruster	8	0.350	-
Pressurant mass	-	15	-
Oxidizer mass	-	328.15	-
Fuel mass	-	196.5	-
Total Dry	-	61	
Total	-	601	-

Table 5.5: Mass sizing

6 | Attitude Control System

6.1. Requirements and Pointing Budget

The attitude control system architecture and sizing is defined from some main requirements coming primarily from the instruments necessary to the scientific investigation. Some of these driving needs are:

ID	Requirements
AOCS-01	The subsystem shall be able to switch mode in a short time, without permanent oscillation around the new stable point
AOCS-02	The subsystem shall be able to shield the payload at all times from solar radiation
AOCS-03	The subsystem shall provide additional dof for the solar array motion to achieve the mission objectives and maintain stable power
AOCS-04	The subsystem shall be able to safeguard the spacecraft in critical conditions through the use of a survival mode
AOCS-05	The subsystem shall be able to desaturate the reaction wheels periodically

Table 6.1: AOCS requirements

The pointing budget in term of accuracy is identified from the various instruments and antennas and reported in table 6.2. In the next section the relevant pointing directions are investigated in the context of the various phases.

6.2. Attitude control modes

The nominal control of the attitude is scheduled by the science events that take place at various position on the nominal orbit, the primary modes are represented in fig. 6.1, and explained in the following list.

Instrument	Accuracy	Mode
ASPERA-4	0.2°	Nadir
MAG	0.25°	Nadir
SPICAV	0.02°	Nadir
HGA	0.5°	Earth pointing

Table 6.2: Accuracy requirements

1. The spacecraft once per orbit will have a low pass near the surface of Venus, during this time the Fine Pointing Accuracy Phase (FPAP) begin. During this phase the satellite pointing direction is Nadir, the spacecraft may also follow dedicated profiles for Venus observation.
2. While further away from the pericenter part of the orbit time is dedicated to communication with Earth. Then a earth pointing attitude phase is initiated, this phase requires a less stringent accuracy than the observation phase.
3. Additionally a Fine Pointing Inertial Phase might be needed for some of the instruments, for example as calibration, this phase will need to use the high accuracy star trackers. This mode will need to point to fixed stars right ascension and declination directions.

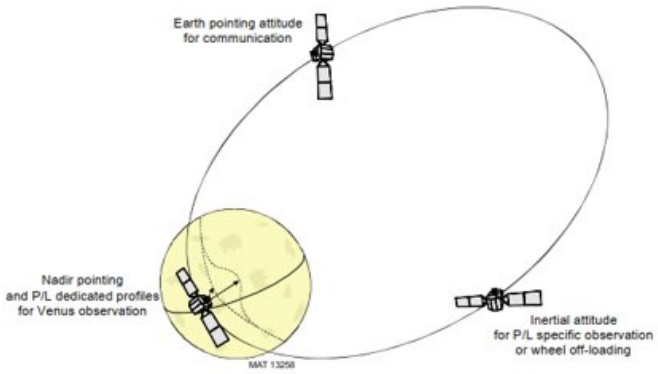

Figure 6.1: Primary attitude control modes

Other secondaries but nevertheless important modes are:

1. The Survival mode, it is initiated each time a critical condition happens and the spacecraft is at risk or has already lost communication or power. This mode is such that no matter what condition the spacecraft has it's prime directive is to re-establish power input from the sun with maximum priority and then try again communication with earth.

2. Another secondary mode is the Reaction Wheel desaturation. During nominal operation reaction wheels are also used to correct for the disturbances on the attitude by various forces, these are usually not periodic and the reaction wheel accumulate angular momentum until saturation. To made them available again for use the RCT thruster must be fired such to remove the angular momentum from the wheels without changing the momentum of the spacecraft.

6.3. Determination of sensors and actuators

The sensors and actuators choice is driven by the requirement of high precision in the observation phase. The following actuator were deemed necessary:

1. Reaction wheels can achieve precise and stable control of the attitude, they will be used for slew during change of phase and to eliminate the effect of disturbances during nominal operations. A skewed configuration is chosen, with the diagonal wheel offering a partial redundancy.

2. Another important set of actuators are the 10N thruster, they are 8, with 4 of them used as a cold redundancy. They are used primarily for orbital control but they are employed also in the aocs s/s for wheel off-loading.

3. The solar array drive mechanism is necessary to achieve the operational attitude without loosing power because of a change in the angle of the solar rays on the arrays. These motors can provide 8 different speed levels and a max rotation of 1.5°/s.

The set of sensors instead is chosen as in the following:

1. Star trackers based on active pixel sensor technology, they are the primary sensor needed for the high accuracy modes, achieving accuracies in the order of arcseconds. They are 2, for redundancy, with a circular fov of 16.4°. They are the same from the Mars express mission with an updated diaphragm to diminish the negative effect of straylight.

2. The sun acquisition sensor are chosen as 2 solar cells mounted on a pyramid, they are derived from the Rosetta and Mars Express mission. They are needed both to obtain a logical signal of the presence of the sun at certain angle and avoid damage to star trackers and additional information on the attitude to orient the solar arrays.

3. The IMU is constituted by two redundant units with 3 accelerometers and 3 gyroscopes. They are used as a secondary source of informations in a Kalman filter with

the star trackers. When the information from the star trackers becomes unavailable they can be used to determine a lower accuracy angular position from gyro drift estimation.

6.4. Perturbations and actuators sizing

A preliminary sizing of the main disturbances affecting the spacecraft's attitude during the orbit in the worst case scenario has been computed.

The main perturbation are the gravity gradient, the Solar Radiation Pressure and the aerodynamic induced torque. Their maximum value and the formulas to calculate them is reported in eq. (6.1).

$$\begin{aligned} T_g &= \frac{3\mu}{2R^3}|I_{max} - I_{min}| = 9.36 \cdot 10^{-4} Nm \\ T_{sp} &= \frac{F_s}{c} A_s (1+q)(c_{ps} - c_g) = 9.07 \cdot 10^{-5} Nm \\ T_a &= \frac{1}{2}\rho C_d A_c v^2 (c_{pa} - c_g) = 1.36 \cdot 10^{-6} Nm \\ T_d &= T_g + T_{sp} + T_a = 0.011 Nm \end{aligned} \tag{6.1}$$

A maximum torque perturbation of 0.011Nm has been estimated and, with margins, this will be the minimum amount of torque that the reaction wheels should be able to provide in each axis. The real reactions wheels of the VEx have a capability of 0.075Nm per wheel, as the surplus effective torque is needed to stabilize the Main Engine during the firing and for the spacecraft overall maneuverability. The slew time needed to do a complete 180° attitude turn can be reverse-engineered.

$$t_{slew}(\theta = \pi) = 2\sqrt{\frac{I_{max} \cdot \theta}{T_{RW} - T_d}} = 369.9s \approx 6min \tag{6.2}$$

Each of this perturbation can either be cyclical or constant during the orbit depending on the attitude. To better estimate the total angular momentum that the reaction wheels need to be able to store a numerical integration over the very eccentric orbit has been computed, eq. (6.3).

$$H = \int_0^T \left(\frac{3\mu}{2} |I_{max} - I_{min}| \frac{1}{R(t)^3} + T_{sp} \right) dt = 9.89 Nms \tag{6.3}$$

The real value of the maximum angular moment that can be stored on the spacecraft is 12 Nms, very similar to our results, and with a good margin of safety.

The procedure to desaturate the wheel involves using the 10 N cold gas thrusters (it is assumed that 2 at a time are used for the calculations). The length of the pulse needed to desaturate a single wheel and the total propellant expenditure over the course of the nominal lifespan of the mission (3 years), considering 3 off-loading maneuvers per orbital period, one for each axis, can be reverse engineered, eq. (6.4).

$$\begin{gathered} T_{thr}(n=2) = n\ F_{thr}\ L_{arm} = 14 Nm \\ t_{pulse} = \frac{H_{RW}}{n\ F_{thr}\ L_{arm}} = 0.86 s \\ Mp_{off} = \frac{n\ F_{thr}\ t_{pulse} \cdot 3 \cdot 365 \cdot 3}{Isp_{thr}\ g_0} \approx 14 kg \end{gathered} \tag{6.4}$$

In the worst case scenario 14 kg of propellant are used to desaturate the wheels during the nominal lifetime. The remaining 46 kg of propellant will be used to perform every once in a while a scheduled apocenter orbit control, since it tends to drift over time, eq. (6.5), fig. 6.2.

$$\Delta v_{left} = Isp_{thr}\ g_0\ \ln\left(1 + \frac{M_{left}}{M_{dry}}\right) = 184.16 m/s \tag{6.5}$$

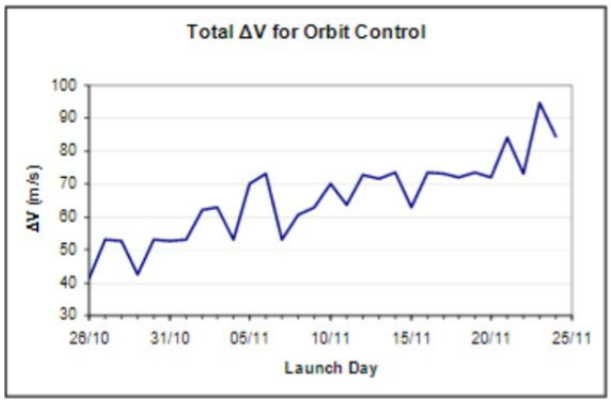

Figure 6.2: Delta-V needed to keep the apogee between 250-400 km for 1000 days

7 | Thermal Control System

7.1. Initial considerations

The Thermal Control System (TCS), like many other subsystems present in the VEx, are derived from the MEx. But while most of them remain substantially unchanged, the TCS was revamped to accomodate for the more difficult environment of the Venusian orbit.

7.2. Requirements

ID	Requirements
HEAT-01	The spacecraft shall maintain at all times a face opposite to the sun light
HEAT-02	All the non radiating surfaces shall be covered with a multi-layer insulation sheets
HEAT-03	The subsystem shall actively maintain the spacecraft temperature in the operational range of the other subsystems and payloads
HEAT-04	The subsystem shall be designed to avoid overheating, in the case where active temperature control is unavailable

Table 7.1: HEAT requirements

7.3. Architecture

The Venus express has two main general heat control architectures, the main one, and the one dedicated to the payload, situated on the -X side of the spacecraft, always supposed to be in the Sun shadow's to avoid overheating. Here the instruments operate on a cryogenic level, needed for the correct functioning of the cameras, thermally separated from the whole structure, with their own radiators.

The main radiators are situated on the faces ±Y, as they are normal to the longitudinal

direction of the solar arrays. This way, when deployed, the Sun rarely will ever impact the radiators, allowing them to dissipate into the deep space.

Everything apart from the solar panels, the instruments and the antennas is covered in MLI, [1], or Multi-Layer Insulation, fig. 7.1a, a lightweight systym of metallic foils able to efficiently repel incoming heat while isolating thermally the spacecraft, fig. 7.1b.

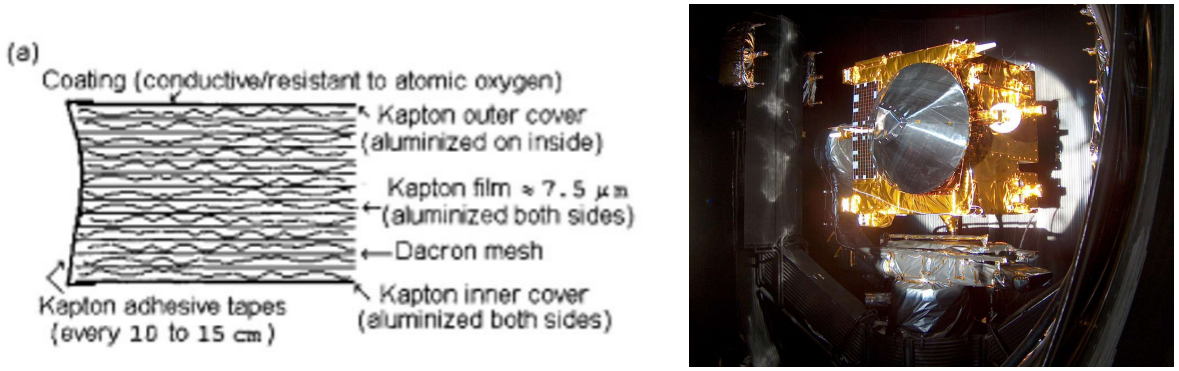

(a) (b)

Figure 7.1: Multi-Layer Insulation schematics and on VEx

Internally, 16 couples of heaters, for redundancy, are distributed within the spacecraft. When needed, electric power is converted to thermal one to heat the modules of interest or the whole spacecraft.

7.4. Environment

The environment of Venus is harsher than the one that the Mars Express previously encountered, as the planet is situated closer to the Sun and the orbit is very elliptical. The heat sources that affect the mission are:

- Solar radiation
- Albedo
- Infrared emission
- Internally generated power

The solar heat flux is dependant on the radius of the irradiated object.

$$\dot{q_{Sun}} = \dot{q_0} \left(\frac{r_{Earth}}{r_{Venus}} \right)^2 \tag{7.1}$$

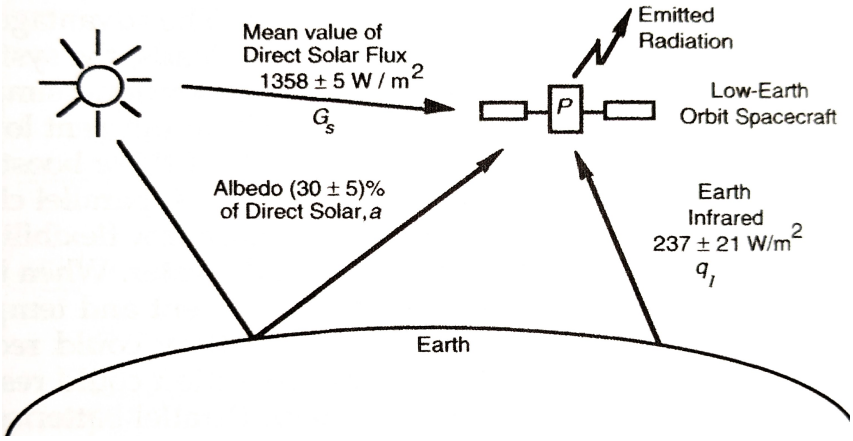

Figure 7.2: Thermal exchange scheme (referred to the Earth)

Where $\dot{q_0} = 1358 \frac{W}{m^2}$ is the standard heat flux that an object orbiting near the Earth receives [4].

The albedo is the fraction of solar heat flux that is reflect by the planet's surface onto our spacecraft. It's dependant on the radius of the planet, the height of the spacecraft and to the albedo factor, a coefficient that estimates how much of the solar heat flux gets reflected into space.

$$\dot{q_a} = \dot{q}_{Sun}\ a_f\ \left(\frac{R_{Venus}}{r_{sc}}\right)^2 \tag{7.2}$$

Venus mean albedo factor is estimated at $a_f = 0.766$ [3].

Venus can be considered as a gray body as it emits a certain fraction of what a black body with that temperature would. Because of Wien's law, $T \cdot \lambda = 2898K \cdot \mu m$, the emission peak is situated in the infrared band. Venus radiative emissions can be modeled with an effective emitting temperature $T_{eff} = 228K$ [3] and an emissivity $\epsilon_{Venus} = 0.68$.

$$\dot{q_{IR}} = \epsilon_{Venus}\ \sigma\ T_{eff}^4 \tag{7.3}$$

Where $\sigma = 5.67\ 10^{-8}\ Wm^{-2}K^{-4}$ is the Stefan-Boltzmann constant.

The electronic components of the spacecraft also dissipate heat, because of Joule's effect, that needs to get expelled into space. A good conservative approximation for the preliminar sizing is to consider the dissipated heat as equal to the spacecraft's payloads peak power consumption $Q_{int} = 427W$ [4].

7.5. Thermal modeling

For the preliminary analysis the system has been modeled with a Lumped Parameters Approach in a single node. The most stringent temperature range (table 7.2) between all the instruments and equipment has been selected as the baseline to not be exceeded, plus margins of safety, table 7.3. The payload ranges have not been included in this calculation as they have a separate independent cooling unit.

Equipment	Operational range	Survival range
Payload VMC	-30°C to 50°C	-50°C to +70°C
Payload Virtis (Visible)	-123°C to +83°C	-
Payload Virtis (Infrared)	-208°C to +183°C	-
Inertial Measurement Unit	-40°C to +71°C	-
Payload SPICAV	-20°C to +40°C	-30°C to +50°C
Electronics	0°C to +40°C	-
Batteries	-5°C to +20°C	-
Solar Arrays	-100°C to +100°C	-165°C to +130°C
Structures	-45°C to +65°C	-

Table 7.2: Temperature ranges for the equipment of the VEx

Max T	Min T
288K	258K

Table 7.3: Identified range with margins

7.5.1. Identification of hot and cold case

A worst case scenario analysis has been run on the hot and cold cases identifiable in our mission. It must be noted that given the high inclination and polarity of the orbit, fig. 7.3, the worst case cold scenario happens during the eclipse, that is always situated near the semi-latus rectum of the orbit.

Once the worst case scenarios have been identificated, a steady-state analysis prior to the sizing of the heaters and the radiators has been run, using a simple balance of energy on the spacecraft, eq. (7.4).

$$\frac{dU(t)}{dt} = \dot{Q}_{Sun} + \dot{Q}_{albedo} + \dot{Q}_{IR} + \dot{Q}_{int} - A_{sc}\epsilon\sigma T^4 = 0 \tag{7.4}$$

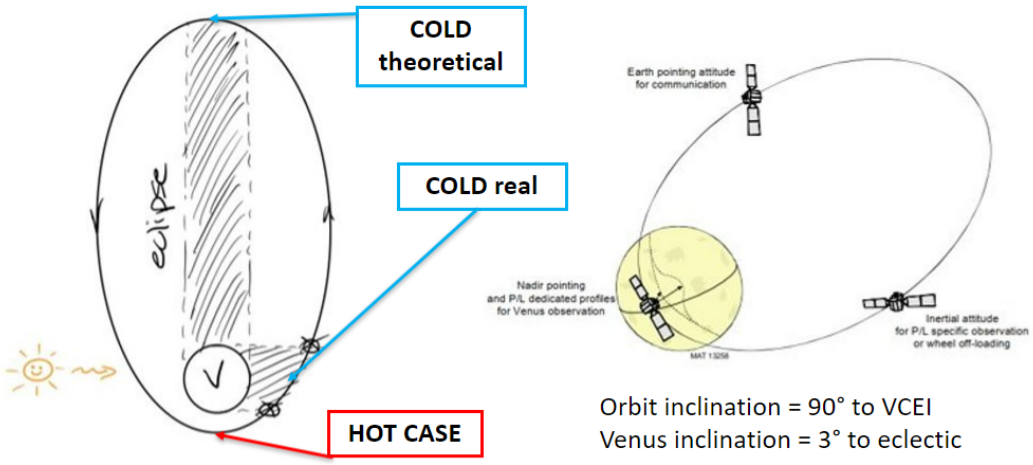

Figure 7.3: Identification of worst case scenarios

With a completely passive system, the temperatures in the worst case scenarios are both too high and too low compared to the acceptable values, table 7.4.

Hot case	**Cold real**	*Cold theoretical*
299K	185K	167K

Table 7.4: Pre-sizing worst case scenarios

7.5.2. Sizing of heaters and radiators

Since the hot case temperature is higher than the maximum acceptable one, radiators are needed to heat the spacecraft during the low temperature phases. The area that the radiators will need to keep the spacecraft in the acceptable ranges is then calculated at the pericenter, the worst case hot scenario, eq. (7.5). The radiators have been approximated with an $\epsilon = 1$, ergo a complete efficiency in heat rejection.

$$\dot{Q}_{Sun} + Q_{alb}(R_{per}) + Q_{IR}(R_{per}) + Q_{int} - (A_{sc} - A_{rad})\epsilon\sigma T_{max}^4 - A_{rad}\sigma T_{hot}^4 = 0 \qquad (7.5)$$

From this, an area of the radiators of 1.74 m^2 has been calculated.

With the radiators present, always dissipating more heat than in the previous case, the cold scenario has been recalculated. The new real cold case has a steady-state temperature of 182K, lower than both the previous cold one and the minimum one. As a consequence,

heaters are needed, and the needed power is calculated, eq. (7.6).

$$Q_{IR}(R_{apo}) + Q_{int} - (A_{sc} - A_{rad})\epsilon\sigma T_{min}^4 - A_{rad}\sigma T_{min}^4 + Q_{heat} = 0 \tag{7.6}$$

A peak power of 2678W has been sized. We can see the comparison with the real world Venus Express in table 7.5.

-	**Radiators area**	**Heater power**
Real Venus Express	$1.7m^2$	781W
Our sizing	$1.74m^2$	2678W

Table 7.5: Comparison between real missing and our sizing

The area of the radiators is very similar, while the power needed by the heaters differs by a lot. This is because the real Venus Express makes use of the fact that the spacecraft never reaches the steady-state cold conditions, as the whole structure acts as a thermal heat sink.

Approximating the thermal properties of the spacecraft with those of an Aluminum metal and running a transient analysis with the heaters off, we can see that in reality the temperature doesn't dip so much, reaching a minimum of only 230K, fig. 7.4.

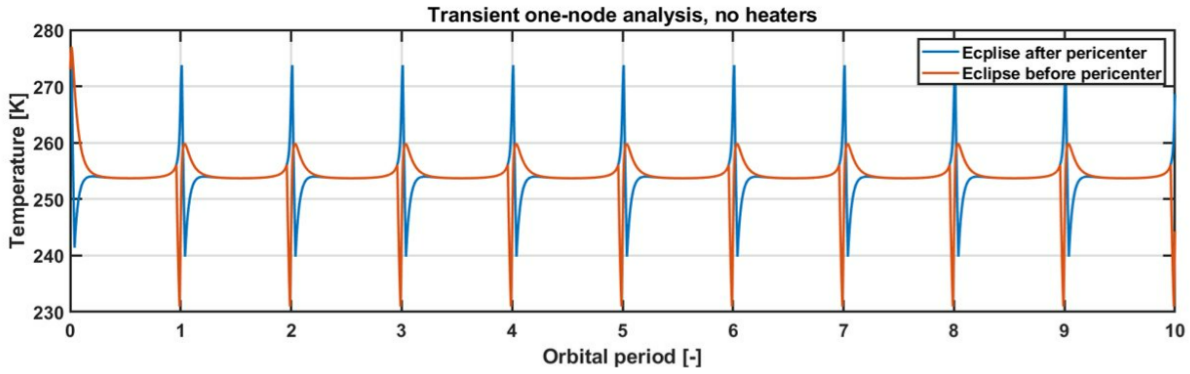

Figure 7.4: Temperature variation during the orbit of Venus, different eclipse cases

As a consequence, we can conclude that the real size of the heaters is lower and our steady-state sizing is unrealistically conservative, while the sizing of the radiators is almost exact.

8 | Electrical Power subsystem

8.1. General Overview

The Venus Express power architecture is shown in fig.8.1b. Electrical power is provided by two solar wings equipped with triple-junction GaAs cells. The array is oriented towards the Sun by two Solar Array Drive Mechanisms (SADMs). When the spacecraft is in an eclipse situation the solar array doesn't generate any power so alternatives have to be considered. In particular, during these situations the power is provided by three lithium-ion batteries that recharge after the eclipse. Power management and regulation is performed by the Power Control Unit (PCU) that provides a regulated 28 V main bus. The PCU uses a Maximum Power Point Tracker (MPPT) in order to operate at the maximum power output of the solar array, which avoids the need to oversize the solar array to cope with both near-Earth and Venus orbit conditions. Battery management is performed using three Battery Charge and Discharge Regulators (BCDRs) under the control of a Main Error Amplifier (MEA) control loop. The resulting +28 V regulated bus is distributed to all spacecraft users by a Power Distribution Unit (PDU) featuring Latching Current Limiters (LCLs), which protect the bus from overcurrents at unit level. The PDU is also responsible for generating the commands for firing the pyrotechnics.

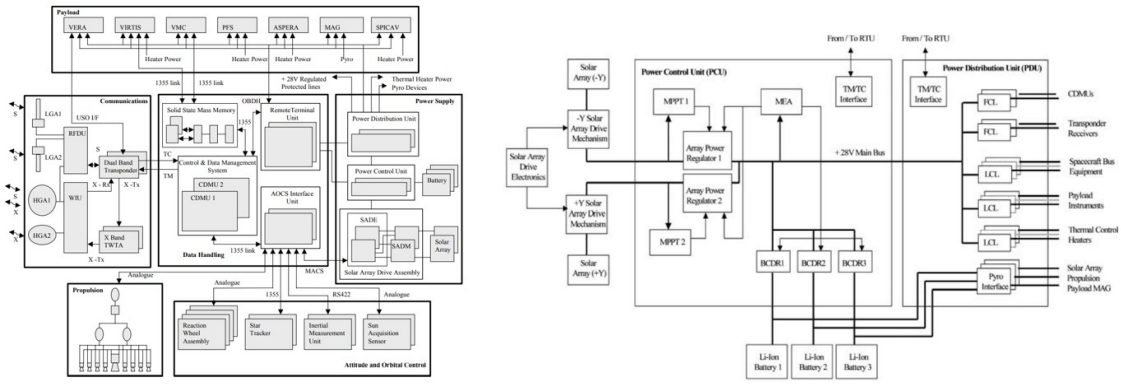

(a) (b)

Figure 8.1: Venus Express power system architecture

8.2. Solar Array

The solar array consists of two identical low-weight deployable wings, each having two solar panels pointed towards the Sun by a one degree-of-freedom SADM. When stowed, each wing was clamped to the spacecraft side panel on four hold-down points and release mechanisms. For deployment (which was performed autonomously after launch as part of the separation sequence), redundant pyrotechnic bolt cutters released each wing individually. The electrical power is transferred to the spacecraft by a harness routed on the rim of the wings onto the connectors of the SADM. In order to meet the stringent requirements associated with the Venus radiation environment, the chosen solar cell technology was GaAs with 100 μm cover glass. The maximum array current is 18 A per wing. The total array power values are of the order of 820 W near Earth and 1400 W at Venus (end-of-life).

8.3. Power storage

Three batteries supply the spacecraft power if either the solar array is not illuminated by the Sun or if the power demand is higher than the one which can be generated by only the array. The energy is stored in three identical 24 Ah low-mass Li-ion batteries with a total capacity of around 500 Wh. Each has 16 parallel strings of six serial 1.5 Ah cells. The batteries are identical to those on Mars Express.

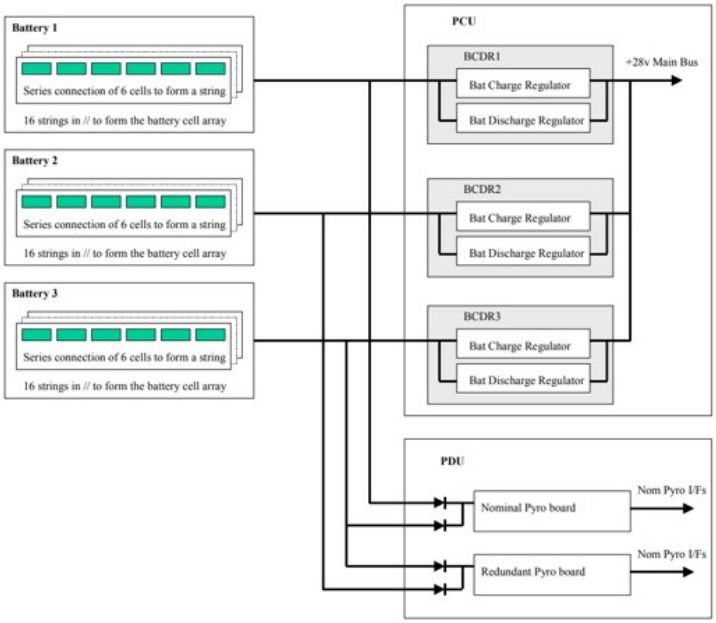

Figure 8.2: EPS power storage configuration

8.4. Power control

The PCU converts the solar array and/or battery power inputs into a regulated main bus voltage of 28 V. The main bus regulation is performed by a conventional three-domain control system, based on one common and reliable MEA signal that controls the two Array Power Regulators (APRs, one for each solar wing) and the three BCDRs (one for each battery). Power management is further achieved by measurement of the power parameters within the PCU itself. When the available array power exceeds the total power demand from the PCU, including the battery power charge, the APR performs the main bus regulation based on the MEA control line signal. In the event that the MEA signal enters either the Battery Charge Regulation or Battery Discharge Regulation domains, the MPPT tracking function automatically takes over. This drives the operating voltage of the solar array to the point where maximum power can be obtained.

8.5. Main bus power distribution

Power distribution is based on a centralised scheme performed by the PDU. One protected power line derived from the regulated main power bus is dedicated to each DC/DC power converter of spacecraft users. In addition, power lines are available for users that draw power directly from the power bus without internal DC/DC conversion, as is the case for the 10 N thruster flow control valves, flow control valves of the main engine coils and of the latch valves. Each power line is switched and protected by an LCL, which is a solid-state switch that also acts as a protection device in case of overcurrent. Units that may never be switched off (CDMU and transponder) have to be able to recover autonomously. For these units, primary power is distributed through Foldback Current Limiters (FCLs). These are devices identical in principle to LCLs except that they do not have ON/OFF switching capability and an overcurrent will not lead to a disconnection when the trip-off time is exceeded. The distribution and the entire system are protected by:

- 78 Latch Current Limiters (LCL): a solid state latching switch which acts as a protection device in case of over current.
- 6 Foldback Current Limiters (FCL): devices similar to LCL, the difference is that they do not feature ON/OFF switching capability
- 32 Pyro lines

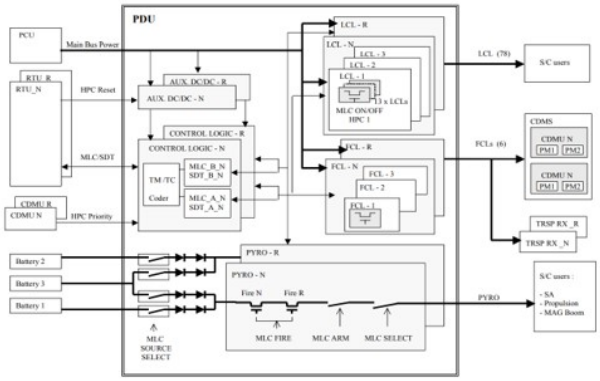

Figure 8.3: EPS power distribution

8.6. Heater distribution

Each Heater Distribution Unit (HDU) consists of a small mechanical box containing printed circuit boards with adjustment resistors for fine tuning the thermal control of the propulsion system. Three HDUs were allocated to nominal propulsion system heater lines and three to redundant heater lines. The maximum power dissipated into each unit does not exceed 14 W.

8.7. Requirements

Some important requirements are shown in tab.8.1:

Id	Requirements
EPS-01	The EP s/s shall be provided with a high degree of autonomy
EPS-02	The primary energy generation component shall maintain adequate energy output for the entirety of the mission
EPS-03	The EP bus shall be fully regulated on a determinate voltage
EPS-04	The solar array shall be able to shift the work point while under variable illumination levels
EPS-05	The batteries shall be able to support a slow charge-discharge cycle and an high DoD

Table 8.1: Electrical power subsystem requirements

8.8. Sizing

Tab.8.2 shows the required power for each scientific payload instruments. The total payload power is obtained by considering the maximum power required by each instrument.

	Power [W]
SPICAV	21 + 10 for 10nm per orbit
VIRTIS	66
PFS	35-45
ASPERA	25
VERA	5
VMC	4
MAG	60
Total Payload Power	235

Table 8.2: Payload power requirements

The power required by each subsystem is then evaluated and presented in tab.8.3. The total subsystem power is considered as the required power in a transmission situation where the power consumption is at the highest values. Considering the maximum power required from the instruments and from the subsystem the EPS should be able to generate at minimum 1122 W. In addition, to size the system in a more correct way also the eclipses have to be taken into account. In particular, the constraints considered are presented in tab.8.4 where the eclipse time is linked to the orbit period.

Subsystem		**Power [W]**
PS	Heater Distribution Unit (HDU) (x3)	42
TTMTC	HGA1 - TWTA	65
	HGA1 - Solid State Power Amplifiers (x2)	10
	HGA2 - TWTA	65
	LGA – Power Handling	10
TCS	Power distributed over 16 redundant heater	695
Total subsystem power		887
Total Power budget		1122

Table 8.3: Total power requirements

Power needed	1122 W
Maximum time in eclipse	1.02 hours
Mimimum time in daylight	22.7 hours
Nominal lifetime	543 days

Table 8.4: Mission contsraints

The chosen technology for the solar array is based on GaAs solar panels while the three batteries on board are 24 Ah low-mass Li-ion batteries. Considering the solar array, the panel efficiency is taken equal to 0.25 whit a efficiency factor in eclipse equal to 0.72 and in daylight equal to 0.82. In addition, an inherent degradation factor of 0.79 is considered for defining the power generated at the beginning of life. Considering now the batteries, the energy efficiency is taken equal to the minimum value for Li-ion batteries which is equal to 0.95. The energy density is taken equal to $150\frac{Wh}{Kg}$. Tab.8.5 shows the results of the sizing with the characteristics mentioned above with respect to the real value of the Venus express.

	Reverse engineering	**Real**
Solar Array		
Beginning Of Life Power [W]	1577	1490
End Of Life Power [W]	1489	1400
Area [m2]	5.4	5.2
Mass [kg]	42.9	41.4
End of life power after 3176 days [W]	1131	[-]
Batteries		
Mass [kg]	22.8	24

Table 8.5: Solar Array and Batteries features

9 | Tracking Telemetry and Telecommand Subsystem

9.1. General Overview

The VEX mission is characterized by different environments during the path from the Earth to Venus and along Venus orbit, in which the spacecraft is able to communicate regularly with Earth's ground stations (Kourou, New Norcia and Cebreros). The trasmission aims to get inputs and to send outputs (telemetry, scientific data, s/s data) in S-band or X-band [9]. Its radio-frequency (RF) communication subsystem consists of a redundant set of dual-band transponders operating in both bandwidths for either the uplink or the downlink. Depending on the mission phase, as better explained in the ConOps paragraph (REF), the transponder is routed via RF switches to different antennas.

The spacecraft has four antennas, which are:

- A dual-band High Gain Antenna (HGA1) operating in S-band and X-band for high-rate telemetry and telecommand;
- A single-band offset HGA2, operating in X-band only, for high-rate telemetry and telecommand;
- Two Low Gain Antenna (LGA), used primarily during Launch and Early Operations Phase (LEOP), operating in S-band for omni-directional reception and hemispherical transmission.

The antennas design and architecture is associated to the one implemented in the Mars Express Mission, used as a baseline for VEX, but with some differences due to the different mission and environments. In particular the LGAs are the same as the one in MEX spacecraft, instead HGA1 has a smaller diameter of 1.3 m with respect to the 1.6 m of MEX to take advantage of the smaller maximum S/C to Earth distance. Moreover, HGA2 antenna has been added for VEX mission to enable S/C communication requirements and to met thermal constraints for the instruments while in orbit around Venus.

9.1.1. Configuration

As could be seen in fig.9.1, the high gain antennas HGA1 and HGA2 are pointing respectively the +X and -X body axis. The low gain antennas LGA1 and LGA2 are pointing respectively +Z and -Z axis.

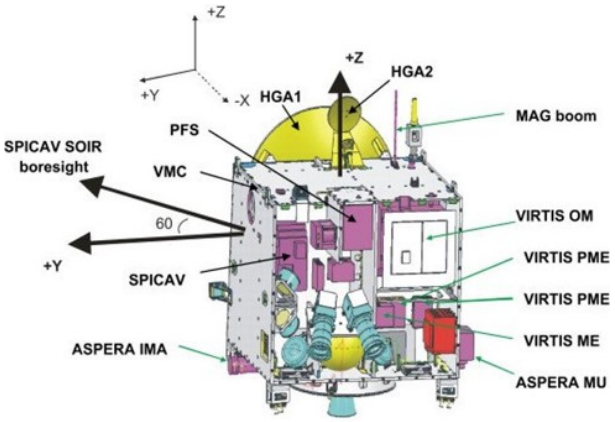

Figure 9.1: Antennas configuration

This configuration has been implemented to minimize the solar illumination of the –X side of the spacecraft (opposite to HGA1) to respect the thermal requirements of the scientific instruments mounted on -X side (VIRTIS and SPICAV).

The steady-state Earth communications ensured by the attitude control let the spacecraft +Z/+X plane remains in the Sun - S/C - Earth plane. This is possible thanks to the 180° relative position of HGA1 and HGA2, that are used respectively depending on the mission phase and, particularly, the relative positions of the Earth, S/C and Venus as shown in fig. 9.2.

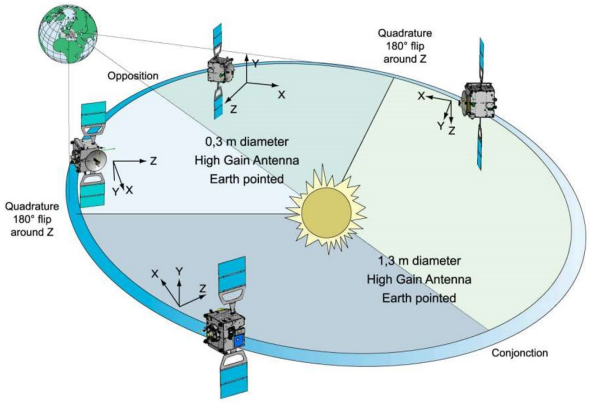

Figure 9.2: Mission phases

The configuration selected for the high gain antennas ensures that during Conjuction

phases, when the S/C is the farest from Earth, the communication is performed by HGA1. Instead, during Opposition phases, when the S/C is closest to the Earth, it is performed by HGA2. In both phases the Sun does not impinge on the lateral sides (±Y sides), moreover the solar panels are always pointed towards the sun with a proper inclination and most importantly the side of the spacecraft that must not be exposed to sunlight (–X side) remains facing cold space.

9.1.2. Schematics

Describing the s/s more in details, the VEX TTMTC is composed by the following components [7]:

- Dual Band Transponder (DBT)
- Radio Frequency Distribution Unit (RFDU)
- Two Travelling Wave Tube Amplifiers (TWTA)
- Waveguide Interface Unit (WIU)
- Four antennas

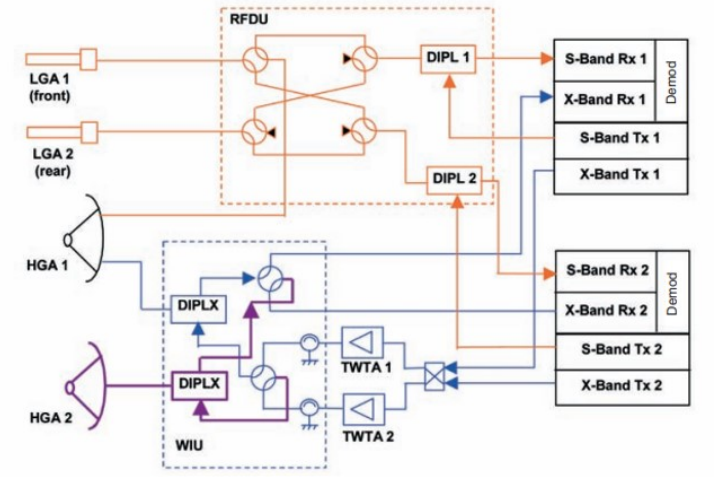

Figure 9.3: TTMTC schematics

In particular the DBT contains two duplicate transmit/receive chains each of which has a transmitter operating in X-Band, a trasmitter with a 5 W final amplifier operating in S-band and an X-Band and a S-band receiver. The X-Band transmitter outputs are connected to the 65-Watt Travelling Wave Tube Amplifiers (TWTAs) via an RF crossover switch. Moreover, the Data Management System is in charge of telemetry data collection

from the spacecraft systems and payload, with an onboard Solid State Mass Memory with a data storage capacity of 12 Gbits.

9.2. ConOps and Data Transmission

The LGAs, which are omnidirectional and operate in S-band, are used during the Launch and Early Operations Phase (LEOP) to communicate with the ground stations. Following LEOP, all nominal operations are performed at X-band, with a downlink capacity up to 228 kbit/s. As mentioned in the Configuration paragraph, the HGA1 is used when Venus is in the superior conjunction side of its orbit and the distance to Earth is the greatest. In order to be able to keep the spacecraft cold face pointed away from the Sun at all times, the HGA2 is used for the portion of Venus's orbit near inferior conjunction (Earth to S/C distances up to 0.78 AU). Then, during Venus Orbit Injection, communications are reverted to S-Band.

The Venus Express orbit can be roughly divided in three parts [10]:

- Pericentre observations (23 – 2 hours orbital time);
- Telecommunications on the descending arc of the orbit (2 – 12 hours)
- Apocentre observations in the ascending arc (12 – 23 hours).

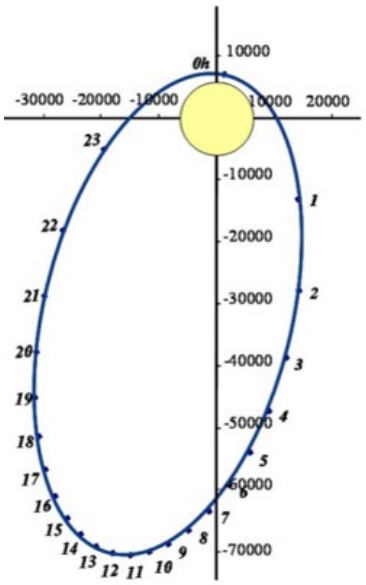

Figure 9.4: Orbit division

The ground station in Cebreros (Spain) is visible from the spacecraft between 2 - 12 hours orbital time, so it's the main GS for data downlink. Data trasmission takes eight hours

and correspond to the downlink of between 100 and 800 megabytes of data, depending on the actual distance between Earth and Venus.

The distance between Earth and S/C affects the time taken to receive the signal, starting from a one-way signal time travel of a few seconds to around 855 seconds when the distance is about 256 million of kilometers.

Moreover, the signal is affected also by the Doppler effect, due to the relative velocity in the direction of the line of sight from Earth to the S/C, which varies from 2.6 to 17.4 km/s. The Doppler effect is analysed with the addition of the Earth rotational speed and measured continuously.

9.3. Requirements

After having analysed the system architecture and evaluated the ConOps, in the table 9.1 the requirements of the s/s are listed:

ID	Requirements
TTMTC-01	The TT s/s shall be modeled on the radio system used on Mars Express
TTMTC-02	The TT s/s shall be configured to provide redundant functions
TTMTC-03	The TT s/s shall be able to perform a two-way and one-way dual-frequency radio link
TTMTC-04	The TT s/s shall be able to work continuously for 8 hours a day
TTMTC-05	The TT s/s shall guarantee the trasmission of 800 Megabyte of data a day
TTMTC-06	Either HGA1 or HGA2 shall be pointed towards Earth during the communication phases
TTMTC-07	Downlink data rate at Venus shall be at maximum 228 kbps
TTMTC-08	The trasponder shall be capable of transmitting and receiving in S-Band and X-Band
TTMTC-09	The Memory Modules shall be enough to guarantee the completation of the nominal mission

Table 9.1: TTMTC requirements

9.4. Sizing

The HGA1 antenna's link budget sizing has been performed through reverse engineering starting from the data publicly available and assuming the unknown ones with proper justifications. It has been decided to perform the sizing of this antenna since is the one mainly used for the communication between S/C and Earth's GS using X-band when the S/C is in operational mode around Venus in the superior conjuction position. Other antenna' sizing has not been performed due to low availability of data and operational conditions.

9.4.1. Link Budget

The known data used for the sizing are reported in the following table 9.2:

Frequency	8.426 GHz
Encoding Method	Convolutional method with 1/2 ratio
Highest data rate	228 kbps
Max distance S/C - Earth	2.6×10^{11} m
Tx antenna diameter	1.3 m
Rx antenna diameter	35 m
Receiver noise temperature	15 K
Efficiency TWTA	0.55
TWTA power	65 W

Table 9.2: Starting Data

Evaluating the link budget for the communication consists into taking into account all the possible losses that the signal could encounter along its path. The main losses are due to transmission (free space, misalignments and atmospheric), cables inside the S/C and noises of the receiver and of the environment. The losses due to the transmission in Space are the highest being equal to -279.18 dB and are related to the signal wavelength and the distance between S/C and receiver. The cable losses are assumed to be -1.5 dB, being on average in that range of values. Assuming an error of alignment equal to 1°, the misalignment losses are equal to -4 dB. Finally, the last loss is given by the signal entering and travelling through the atmosphere, where an elevation angle of the signal as been approximated to 10°, the loss is equal to -2 dB evaluated graphically from atmospheric models.

The gain of the transmitter is given mainly by its diameter, efficiency (in this case taken equal to the TWTA efficiency), and the wavelenght of the signal. The HGA1 antenna of Venus Express has a gain of 38.6 dBm. Using the gain, the cable losses and the real power of the transmitter is possible to evaluate the EIRP, equal to 82.64 dBm. Knowing the gain of the receiver, which is calculated in the same way of the TX one, it's possible to compute the receiver power, in order to finally obtain the link budget.

Since VEX TTMTC system uses a convolutional encoding method with 1/2 ratio, and assuming a bit per error rate (BER) equal to 10^{-5} typical of scientific data, it is expected to have a theoretical Eb to N0 ratio (link budget) equal to 4 dBm (graphically).

The link budget obtained by the calculations, taking into account the thermal noise at the receiver, is equal to 24.82 dBm, higher than the theoretical one given the different assumptions made along the calculations algorithm.

10 | Conclusions

In conclusion, the Venus Express mission was a pioneering endeavor that allowed for a comprehensive study of the planet Venus. The reverse engineering analysis of all the subsystems of the spacecraft revealed valuable insights into the design, functionality, and performance of the mission's hardware and software.

Through a preliminary sizing the design choices and values were checked and the results were very similar to the real mission, confirming the accuracy of the design.

The mission's ability to successfully operate in the harsh environment of Venus, and its prolonged longevity, demonstrated the robustness and adaptability of the spacecraft's systems. The scientific data collected by Venus Express provided a new understanding of Venus's atmosphere, geology, and potential for habitability, and will continue to be a valuable resource for researchers.

The Venus Express mission was a remarkable achievement in space exploration, and the analysis of the spacecraft's subsystems has added to our understanding of the mission's technical accomplishments.

Bibliography

[1] Heat transfer through multi-layer insulation (MLI). *Physica C: Superconductivity and its Applications*, 583:1353799, 2021. ISSN 0921-4534.

[2] C. J. Hunter. Venus Express Chemical Propulsion System. The Mars Express Legacy. *4th Int. Spacecraft Propulsion Conference*, Oct. 2004.

[3] L. V. Ksanfomaliti. Infrared thermal radiation of Venus. *USSR Report Space*, 22(2): 77, Jan. 1984.

[4] W. J. Larson and J. R. Wertz. *Space Mission Analysis and Design*. Microcosm Inc., 2nd edition, 1992.

[5] J. M. S. Pérez. Venus Express Spacecraft Design Report. *European Space Operations Centre*, Feb. 2004.

[6] J. M. S. Pérez. Venus Express: Consolidated Report On Mission Analysis. *European Space Operations Centre*, Apr. 2005.

[7] P. Sivac and T. Schirmann. The Venus Express Spacecraft System Design.

[8] G. P. Sutton. *Rocket Propulsion Elements*. John Wiley, 9th edition, 2017.

[9] H. Svedhem and D. Titov. Venus Express mission. *Journal of Geophysical Research Atmospheres*, Jan. 2005.

[10] H. Svedhem and D. Titov. Venus Express science planning. Apr. 2006.